Available online at www.sciencedirect.com

ScienceDirect

Energy Procedia 59 (2014) 315 – 322

Energy Procedia

European Geosciences Union General Assembly 2014, EGU 2014

Combining numerical modeling with geostatistical interpolation for an improved reservoir exploration

Wolfram Rühaak[a]*, Kristian Bär[b], Ingo Sass[b]

[a]*Technische Universität Darmstadt, Graduate School of Energy Science and Engineering, Jovanka-Bonschits-Strasse 2, 64287 Darmstadt*
[b]*Institute of Applied Geosciences, Department of Geothermal Science and Technology, Schnittspahnstr. 9, D-64287 Darmstadt, Germany*

Abstract

Subsurface temperature is one of the key parameters in geothermal exploration. The estimation of the reservoir temperature is of high importance and usually done either by interpolation of temperature data or numerical modeling. However, temperature measurements of depths larger than a few hundred meters are generally very sparse. A pure interpolation of such sparse data always involves big uncertainties and usually neglects knowledge of the reservoir geometry or reservoir properties.
Kriging with trend does allow including secondary data to improve the interpolation of the primary one. Using this approach temperature measurements of depths larger than 1,000 m of the federal state of Hessen/Germany have been interpolated in 3D. A conductive numerical 3D temperature model was used as secondary information. This way the interpolation result reflects also the geological structure. As a result the quality of the estimation improves considerably.

Peer-review under responsibility of the Austrian Academy of Sciences

Keywords: Subsurface temperatures; Kriging with External Drift; Finite Element Modeling

Nomenclature

λ	thermal conductivity (W m^{-1} K^{-1})
T	temperature (°C)
H	heat sinks and sources (W m^{-3})

* Corresponding author. Tel.: 49 6151 16-3671; fax: +49 6151 16-6539.
E-mail address: ruehaak@geo.tu-darmstadt.de

Peer-review under responsibility of the Austrian Academy of Sciences
doi:10.1016/j.egypro.2014.10.383

1. Introduction

An important task in geoscience is the interpolation of scattered spatial data. Prediction of subsurface temperatures (typically 1 km – 5 km depth) is of special relevance for geothermal exploration. Knowledge about the actual subsurface temperatures is critical [1]; for a geothermal project 10 °C more or less can mean the difference between success and failure. Any available information should therefore be included. In contrast to more simplified 2D approaches we promote the application of full 3D studies.

Since subsurface temperature data for great depths are typically sparse, different approaches for estimating the spatial subsurface temperature distribution are tested. A promising approach is kriging with external drift (a specific case of kriging with a trend model) where a geostatistical (kriging) interpolation is combined with a numerical result. Similar approaches have been performed before with other properties like groundwater heads [2], but to our knowledge never with subsurface temperatures.

2. 3D Kriging of Temperature Measurements

For predicting subsurface temperatures different interpolation methods can be applied. Besides other approaches ordinary and universal kriging have been applied in various studies (e.g. [3], [4], [5], [6], [7]). Kriging is the name for a group of interpolation methods for which an unknown value of a regionalized variable (a random field) is estimated under consideration of the spatial structure given by the variogram. The spatial properties of the data are taken into account by the variogram. Based on the variogram, a mathematical model function is estimated which reflects the spatial correlation. This model function is used as weight by the kriging procedure. Additionally, kriging gives information about the error of the estimation.

Different qualities of the data are related to subsurface temperature measurements taken in boreholes where the original subsurface temperature is disturbed due to the drilling process. After correction of the data, a substantial, only roughly known error still persists. One simple option is of course to exclude such values of lower quality. This is inevitable for some obviously wrong data. However, subsurface data are typically sparse and it is therefore better to use poor data where no other data exist. This is one of the benefits of the algorithm presented here.

2.1. Ordinary Kriging

Ordinary kriging is the most general and widely used kriging method for stationary processes. It assumes a constant but unknown mean. Given n measurements of z at locations with spatial coordinates x_1, x_2, ..., x_n, the value of z at point x_0 can be estimated with [9]:

$$\hat{z}_0 = \sum_{i=1}^{n} w_i z(\mathbf{x}_i) \tag{1}$$

Hence w_i is the weight which has to be determined for this linear estimator. The kriging system can be written as (see e.g. [10]; [9]; [11]; [12]):

$$\begin{bmatrix} \mathbf{A} & \mathbf{1}_n \\ \mathbf{1}_n^T & 0 \end{bmatrix} \mathbf{w} = \mathbf{b}\,, \tag{2}$$

where $\mathbf{A}$ is a n times n matrix with element A{i, j} equal to the variogram functions $-\gamma(\mathbf{x}_i - \mathbf{x}_j)$, recalling that $\gamma(0) = 0$, $\mathbf{1}_n$ is a vector of length n of ones, $\mathbf{w}$ is a vector of length n+1 the first n elements being kriging weights w_1, w_2, …, w_n and the last element of which is a Lagrange multiplier ν, and $\mathbf{b}$ is a vector of length n+1 with the i^{th} element equal to $-\gamma(\mathbf{x}_i - \mathbf{x}_0)$ for $i \leq n$ and the n^{th} element set to 1. Solving this system, w_1, w_2, ..., w_n are obtained, which are the linear estimators of Eq. 1. Additionally the mean square estimation error can be calculated.

2.2. Kriging of erroneous data

If the data have an error, which can be quantified, it is possible to take this information into account similar to a regression-model [13]:

$$\hat{z}_0 = \sum_{i=1}^{n} w_i \left[z(\mathbf{x}_i) + \varepsilon(\mathbf{x}_i) \right], \tag{3}$$

where the error $\varepsilon(\mathbf{x}_i)$ has a known variance $\mathrm{Var}[\varepsilon(\mathbf{x}_i)] = \sigma^2_i$. For solving, the regular kriging system is computed except for the diagonal terms, in which the variances of the measurement error are included in the main diagonal of the matrix:

$$\mathbf{A}_{\varepsilon} = \mathbf{A} - \begin{bmatrix} \mathrm{diag}(\sigma^2) & \mathbf{0}_n \\ \mathbf{0}_n^T & 0 \end{bmatrix} \tag{4}$$

A code called jk3d† has been programmed using JAVA which computes an according modified ordinary kriging solution [7].

3. Subsurface Temperature Data

Most of the data come from undisturbed continuous logs (measured when boreholes were at temperature equilibrium), but with a sparse lateral distribution. The accuracy of continuous logs is estimated to be ±0.01 °C [14]. The remaining data are bottom hole temperatures (BHT) or temperature data from drill stem tests (DST). The BHT data have a much larger spatial (especially lateral) distribution than all the other temperature values, but the quality of BHT measurements is poor because they are carried out during the drilling process when the thermal field is not in equilibrium. The accuracy of corrected BHT values depends on the applied correction method; measurement errors between ±3 °C and up to ±5 °C-10 °C are presumed [14] [15]. However, the real measurement error is unknown. Based on the quality of the data, a respective measurement error is estimated and shown in Table 1 (for details see [16]; [17]; [7]).

In this study the global trend value (geothermal gradient) is removed from the data for variogram modeling and the subsequent kriging and finally added to the kriging results again. For the linear regression the surface temperature is assumed to be constant at 5 °C.

4. Variograms

A difficult but important part is to derive good variograms for the horizontal and vertical direction. The variograms give necessary information about the spatial dependence of the data. The horizontal variogram is based on all data from the Odenwald and Sprendlinger Horst (ODW), Hanau Seligenstädter Senke (HSS), Hessen North-East (NE) and Schiefergebirge (RH) submodels. Data from the Mainzer Becken (MZ) and the Oberrheingraben (ORG) submodels are not used for this variogram as they are strongly convectively disturbed. The vertical variogram is based on data from all regions but only high quality measurements from continuous logs are used.

The calculated experimental variograms and the fitted functions are shown in Fig. 2. The variograms are calculated based on the residual temperature data where the trend is removed. The result for the horizontal direction is shown in the left of Fig. 2. Due to the high geological heterogeneity the result is quite poor, but it is still possible to fit a theoretical variogram to the data.

† http://sourceforge.net/projects/jk3d/

With the complete data-set it is not possible to obtain a reasonable experimental variogram for the vertical direction. However, if solely the high quality continuous logs are used, with data only from depths larger than 250 m, the result is substantially better (Fig. 2 right). As the horizontal distribution of these log data is very sparse it is not possible to calculate a horizontal variogram based on these data only. The vertical variogram shows a clear non-stationary progression from 250 m on, which is neglected for the modeled variogram; at interpolation this is considered due to a search radius limited to 200 m. The fit for the horizontal case is obviously poor. However, a perfect fit is in general not necessary [9]; a qualitative fit is mostly sufficient. The estimated values for the range are comparable to the values estimated by [5] for the Provence basin, of horizontal 23 km and vertical 500 m.

Table 1. Description of the different subsurface temperature measurements.

Code	Measurement Description	Estimated Error ε (K)	Number
1	undisturbed logs	0.01	1360
2	disturbed temperature logs	2.4	200
11	BHT with at least 3 temperature measurements taken at different times in the same depth; corrected with a cylinder -source approach	0.5	58
21	Production test (DST)	0.5	
12	BHT with at least 2 temperature measurements taken at different times in the same depth; corrected using the Horner -plot method	0.7	85
13	BHT with at least 2 temperature measurements taken at different times in the same depth; corrected with an explosion line-source approach	0.7	
14	BHT with one temperature measurement, known radius and time since circulation (TSC)	1.6	46
15	BHT with one temperature measurement, known TSC	1.6	
16	BHT with one temperature measurement, known radius	3	280
17	BHT with one temperature measurement, unknown radius and unknown TSC	3	

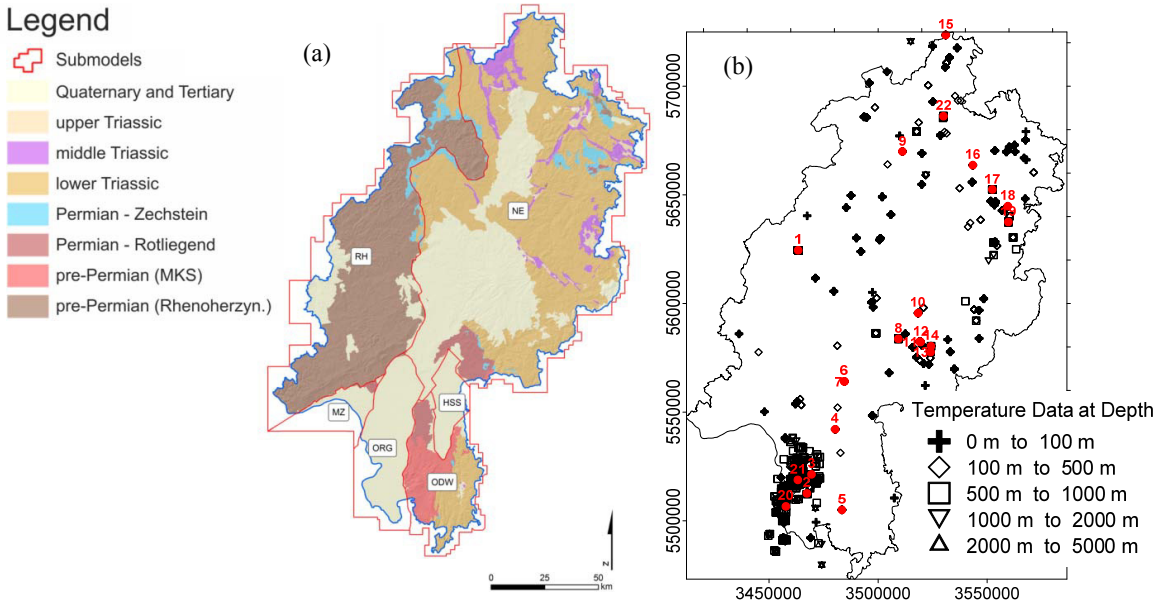

Fig. 1 (a) Submodels within the 3D model of the federal state of Hessen; for abbreviations see text; (b) locations with temperature data (modified after [19]); the 22 available logs which are used for validation are marked with red labels and numbers.

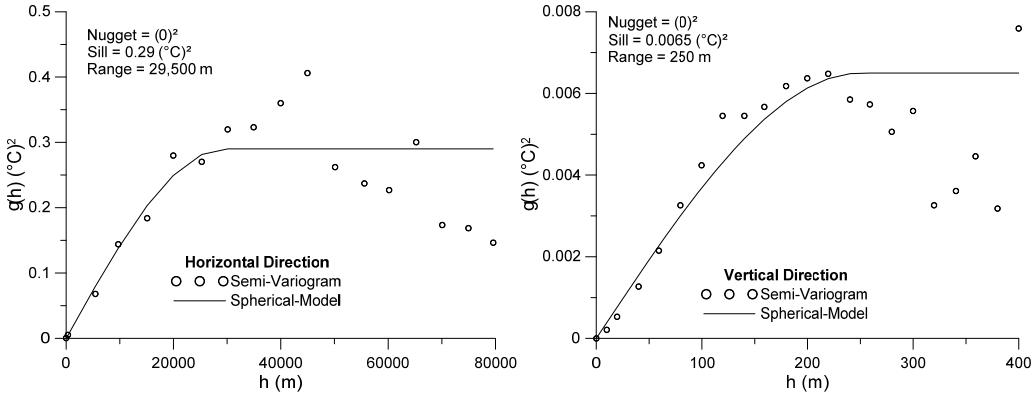

Fig. 2 Horizontal and vertical experimental and theoretical variograms for the residual temperature data.

5. Numerical Modeling

A classical approach for estimating the subsurface temperature distribution is the numerical computation of a 3D purely conductive steady state temperature distribution.

Based on a 3D structural GOCAD model [18] and an extended geothermal database [19] of the federal state of Hessen/Germany the subsurface temperature distribution is computed.

The 3D finite element mesh with layers for all geological units is constructed by converting the original Hessen 3D GOCAD Model ([19], [20]). The thermal conductivity described in [19] is assigned to the respective units (see Table 12). No calibration was performed. On the surface long term yearly average temperatures (data from the German Meteorological Service, DWD) are assigned as Dirichlet boundary conditions. A basal heat flow is estimated following the approach of [18]. It is spatially varying from 65 mW m^{-2} to 95 mW m^{-2} according to the presumed Moho depth using data from [21].

Several codes are available for the numerical solution [22]. Here the software FEFLOW [23] was used. Only conductive heat transfer is considered as not enough data for convective heat transport at great depths are available. The paleoclimatic disturbances of the temperature (e.g. [24]) are also not considered; furthermore internal heat sources are neglected. The solution therefore simplifies to:

$$\nabla \cdot \left(\boldsymbol{\lambda} \nabla T \right) = 0 \tag{5}$$

The model is validated using the available continuous temperature-logs. The fit of the modeled logs is very good in areas which are not influenced by convection, within such areas the fit is poor.

Table 2. Assigned values for the numerical model.

Nr	Modell Unit	Porosity n (-)	λ (W m^{-1} K^{-1})
1	Tertiary (Vulcanite)	0.016	1.84
2	Triassic Muschelkalk	0.043	2.10
3	Triassic Buntsandstein	0.135	2.97
4	Permian Zechstein	0.115	2.55
5	Permian Rotliegend	0.089	2.42
6	N‘ basement metamorphic.	0.036	2.81
6	S‘ basement crystalline	0.002	2.40

6. Kriging with External Drift

Kriging with an external drift (KED) is a variant of universal kriging, or kriging with a trend model (KT) [25]. KED is a simple and efficient algorithm to incorporate a secondary variable in the estimation of the primary variable. However, the fundamental relation must make sense in terms of the underlying physics.

The trend m(u) is modeled as a linear function of a smoothly varying secondary (external) variable f_k, instead of as a function of the spatial coordinates, like in kriging with a trend model. f_k is assumed to reflect the spatial trends of the z variability up to a linear rescaling of units. The estimate of the variable and the corresponding system of equations are identical to the kriging with a trend model [25]. Now for the KT estimator the full kriging with trend system can be written as [26]:

$$\begin{bmatrix} [\gamma(\mathbf{x}_i - \mathbf{x}_j)] & [f_k(\mathbf{x}_i)]^T \\ [f_k(\mathbf{x}_j)] & [0] \end{bmatrix} \begin{bmatrix} [w(\mathbf{x})]^T \\ [\nu(\mathbf{x})]^T \end{bmatrix} = \begin{bmatrix} [\gamma(\mathbf{x}_i - \mathbf{x})]^T \\ [f_k(\mathbf{x})]^T \end{bmatrix} \tag{6}$$

$f_k(\mathbf{x})$ are secondary data which have to be known for all grid nodes and all observation points. For further details see [25].

Additionally, similar to the ordinary kriging, the measurement error is considered in the study presented here by adding a variance to the main diagonal of the left-hand side matrix.

For this study the same settings like for ordinary kriging have been applied for kriging with external drift; using an extended version of jk3d the result of the numerical model was added as drift variable by interpolating the result to all mesh nodes and data points, by using an inverse distance weighted interpolation.

The KED result showed at some locations at the border anomalous temperatures. For stabilizing the solution several artificial temperatures according to the geothermal gradient were added, but only outside of the solution domain; additionally a very large measurement error of 25 °C is assigned which reduces the impact on the solution further.

7. Results

In Fig. 3 and Fig. 4 the results for ordinary kriging, the conductive numerical model and kriging with external drift are shown for a depth below the surface of 500 m and 1000 m, respectively.

For the ordinary kriging and the kriging with external drift a modified approach is applied where the quality of the temperature measurements is taken into account [7]. Though the data are distributed too sparse for evaluating the total area using ordinary kriging, no blanking is applied, to make the comparison with the two other results easier.

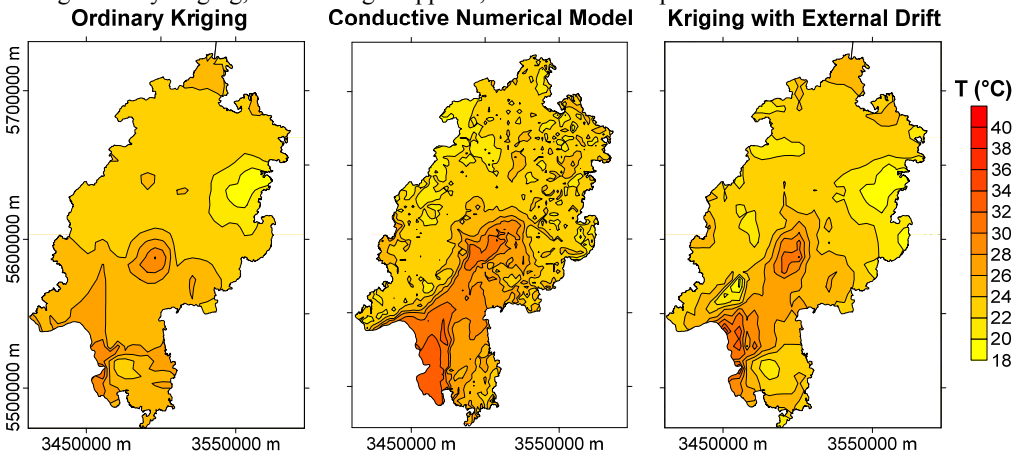

Fig. 3 Comparison of kriging, numerical modeling and kriging with external drift results in 500 m depth below the surface.

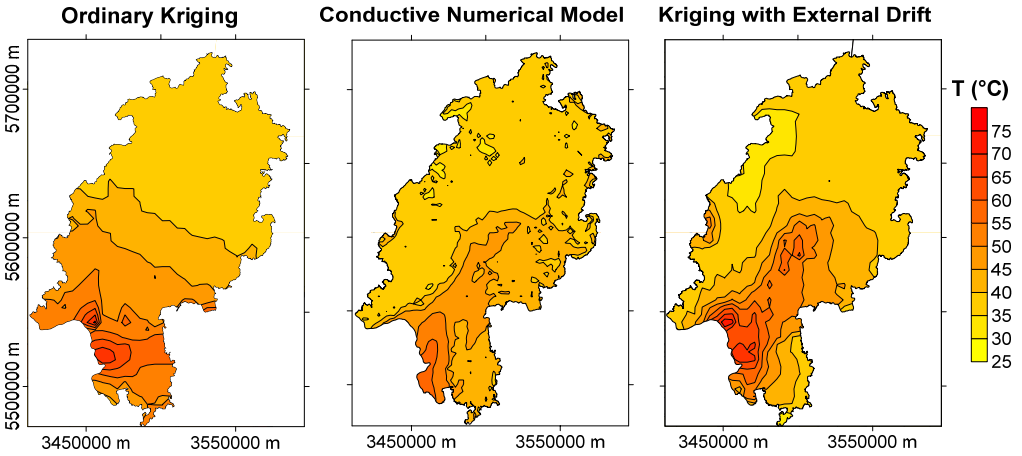

Fig. 4 Comparison of kriging, numerical modeling and kriging with external drift results in 1,000 m depth below the surface.

The results reveal that the ordinary kriging result indicates nicely the effect of temperature anomalies due to convective groundwater flow, especially in the south in the Upper Rhine Graben at a depth of 1,000 m; however the layering of the different geological units is not considered. In difference the purely conductive numerical result shows clearly the effect of the layering of the geological units but calculated temperatures in the Upper Rhine Graben are significantly lower than the measured values. The model result which uses the original values from [19] without any modifications, gives a very good fit with most continuous temperature logs. However, it fails in predicting the temperatures in regions with stronger convective heat transport.

Finally the result of kriging with external drift combines the numerical result with the geostatistical interpolation. This way the subsurface temperature is predicted using all information available.

8. Discussion and Conclusions

Differences in the predicted subsurface temperature distribution are mainly related to convective processes, which are reflected by the interpolation result, but not by the numerical model. Therefore, a comparison of the two results is a good way to obtain information about flow processes in such great depths. This way an improved understanding of the heat transport processes within the presented low-mid enthalpy geothermal reservoir (500 m – 6000 m) is possible.

The computation of a fully coupled flow and heat transport model would be ideal. However, due to the small number of data and missing full understanding of convective heat transport along faults any such result lacks of reliability.

Obtaining the theoretical variograms necessary for kriging is a difficult task. Especially the quality of the horizontal semi-variogram is poor. However, it is sufficient for obtaining a reasonable spatial temperature distribution. Especially the inclusion of a weighting algorithm [7] helps to improve the Kriging result as artefacts due to low quality measurement only have a small impact - where high quality data are available.

The combination of both approaches might result in a temperature model with a good fit to the given temperature measurements as well as a good extrapolation of subsurface temperatures in depths where no data is available. Such a model increases the quality of geothermal potential predictions compared to purely numerical or geostatistical approaches.

In this study the paleoclimate signal was not taken into account, which is especially relevant for depths up to approximately 1,000 m. Also heat production was neglected for the numerical model. Both aspects as well as the influence of fault zones as conduits for convective heat transport should be addressed in future work. Additionally the impact of a temperature dependent thermal conductivity should be addressed.

Acknowledgements

This work is supported by the DFG in the framework of the Excellence Initiative, Darmstadt Graduate School of Excellence Energy Science and Engineering (GSC 1070).

References

[1] Huenges E, Kohl T, Kolditz O, Bremer J, Scheck-Wenderoth M, Vienken T. Geothermal energy systems: research perspective for domestic energy provision. Environmental Earth Sciences 2013;70(8): 3927-3933.
[2] Rivest M, Marcotte D, Pasquier P. Hydraulic head field estimation using kriging with an external drift: A way to consider conceptual model information. Journal of Hydrology 2008;361(3-4): 349-361.
[3] Chilès JP, Gable R. Three dimensional modelling of a geothermal field. In: Geostatistics for natural resources characterization, Part 2, D. Hingbam, MA: Reidel Publish. Comp; 1984. p. 587-598
[4] Bonte D, Guillou-Frottier L, Garibaldi C, Lopez S, Bourgine B, Lucazeau F, Bouchot V. Subsurface temperature maps in French sedimentary basins: new data compilation and new interpolation. Bull Soc Gol Fr 2010;181(4):377-390.
[5] Garibaldi C, Guillou-Frottier L, Lardeaux JM, Bonte D, Lopez S, Bouchot V, PL. Relationship between thermal anomalies, geological structures and fluid flow: new evidence in application to the Provence basin (southeast France). Bull Soc Gol Fr 2010;181(4):363-376.
[6] Agemar T, Schellschmidt R, Schulz R. Subsurface temperature distribution in Germany. Geothermics 2012;44(0):65-77.
[7] Rühaak W. 3-D interpolation of subsurface temperature data with measurement error using kriging. Environmental Earth Sciences 2014; in press.
[8] Matheron G. Les variables régionalisées et leur estimation: une application de la théorie des fonctions aléatoires aux sciences de la nature. Paris: Masson; 1965.
[9] Kitanidis PK. Introduction to Geostatistics, Applications in Hydrogeology. Cambridge: Cambridge University Press; 1997.
[10] Isaaks EH, Srivastava RM. An Introduction to Applied Geostatistics. Oxford : Oxford University Press; 1989.
[11] Chilès J, Delfiner P. Geostatistics: Modeling Spatial Uncertainty. New York: Wiley; 1999.
[12] Davis JC. Statistics and Data Analysis in Geology, 3rd Edition. New York: Wiley; 2002.
[13] Delhomme J. Kriging in the hydrosciences. Advances in Water Resources 1978;1(5);251-266.
[14] Bächler D, Kohl T, Rybach L. Impact of graben-parallel faults on hydrothermal convection - Rhine Graben case study. Phys Chem Earth 2003;28(9-11):431-441.
[15] Goutorbe B, Lucazeau E, Bonneville A (2007) Comparison of several BHT correction methods: a case study on an Australian data set. Geophys J Int 170:913–922
[16] Rühaak, W: A Java application for quality weighted 3-d interpolation. Computers & Geosciences 2006;32,1.
[17] Rühaak W, Rath V, Clauser C: Detecting thermal anomalies within the Molasse Basin, Southern Germany. Hydrogeology Journal 2010;18(8):1897-1915.
[18] Arndt D, Bär K, Fritsche J-G, Kracht M, Sass I, Hoppe A. 3D structural model of the Federal State of Hesse (Germany) for geo-potential evaluation. Z. Dt. Ges. Geowiss. 2011;162(4):353-369.
[19] Bär K, Arndt D, Fritsche J-G, Götz AE, Kracht M, Hoppe A, Sass I. 3D-Modellierung der tiefengeothermischen Potenziale von Hessen - Eingangsdaten und Potenzialausweisung. Z. Dt. Ges. Geowiss. 2011;162(4):371-388.
[20] Sass I, Hoppe A, Arndt D, Bär K: Forschungs- und Entwicklungsprojekt 3D Modell der geothermischen Tiefenpotenziale von Hessen. Report, Technische Universität Darmstadt; 2011.
[21] Dézes P, Ziegler PA. European Map of the Mohorovičić discontinuity. In: Mt. St. Odile, 2nd EUCOR-URGENT Workshop (Upper Rhine Graben Evolution and Neotectonics), France. 2001.
[22] Anderson MP. Heat as a ground water tracer. Ground Water 2005;43(6):951-968.
[23] Diersch H-J. Finite Element Modeling of Flow, Mass and Heat Transport in Porous and Fractured Media. Heidelberg: Springer; 2014.
[24] Hartmann A, Rath V. Uncertainties and shortcomings of ground surface temperature histories derived from inversion of temperature logs. J. Geophys. Eng. 2005;2(4):299.
[25] Deutsch CV, Journel AG. GSLIB: Geostatistical Software Library and Users's Guide. 2nd ed. Oxford: Oxford University Press; 1998.
[26] Webster R, Oliver MA. Geostatistics for Environmental Scientists. 2nd ed. Chichester: John Wiley & Sons; 2007.